ARTICLE IN PRESS

Ocean Engineering xxx (xxxx) xxx

Contents lists available at ScienceDirect

Ocean Engineering

journal homepage: www.elsevier.com/locate/oceaneng

Loss of lock-in in VIV due to spanwise variations of diameters

S. Bahramiasl [a,b,*], E. de Langre [a]

[a] LadHyX, Ecole Polytechnique, Institut Polytechnique de Paris, CNRS, Palaiseau, France
[b] Department of Mechanical Engineering, Sharif University of Technology, Tehran, Iran

ARTICLE INFO

Keywords:
Vortex induced vibration wake oscillator model
linear stability diameter ratio

ABSTRACT

Elongated cylindrical structures with non-uniform diameters, under cross-flow, are often encountered in marine engineering and energy harvesting devices. In this work, the vortex-induced vibrations of elastically supported circular tapered and wavy cylinders with different cross sections areas are studied numerically using a wake oscillator model. The effect of the tapering ratio on the amplitude of oscillation is particularly analyzed. For tapered cylinders it is found that the amplitude of oscillation under flow decreases strongly when a critical tapering is reached. This is consistent with experimental data. A similar effect is found in wavy cylinders. A third system, consisting of a two-section cylinder, also elastically supported and under cross-flow is then considered and the drop in amplitude is related to the ratio between diameters. For this system, a linear stability analysis of the equations of the coupled fluid-solid system allows giving a good approximation of the critical diameter ratio, consistently with the tapered cylinder case. It is concluded that the critical diameter ratio corresponds to the maximum variation in vortex shedding parameters that the coupled wake-cylinder system can support along its length while keeping a consistent vortex shedding.

1. Introduction

Vortex Induced Vibration (VIV) is a form of coupling between a wake and an elastic structure (Williamson and Govardhan, 2004). It might lead to fatigue, but is also a way to harvest energy by flows (Grouthier et al., 2014). Cylinders undergoing VIV may not be of uniform cross-section. Tapered and wavy cylinders have been studied in the past. For tapered cylinders (Fig. 1(a)) several authors (Bargi et al., 2015; Hover et al., 1998; Kaja et al., 2016; Techet et al., 1998; Seyed-Aghazadeh et al., 2015; Zeinoddini et al., 2013) have shown that a strongly tapering almost suppresses VIV. In their work different cylinders in terms of mass ratios and tapering ratios have been studied numerically and experimentally. Differences and similarities have been found between linearly tapered cylinders subject to uniform flow and uniform cylinders subject linearly sheared flow (Balasubramanian and Skop, 1996; Parnaudeau et al., 2007). Balasubramanian showed a similar oscillating behavior for the two cases. Some authors analyzed the cellular vortex shedding for a tapered cylinder (Mathelin and De Langre, 2005; Narasimhamurthy et al., 2009). For wavy cylinders Fig. 1(b), the wake and in consequence VIV are also affected by the amplitude and wavelength of the waviness, as well as the heading angle in elliptical wavy cylinders. (Balasubramanian and Skop, 1996; Lam et al., 2004; Lam and Lin, 2009; Lee and Nguyen, 2007; Zhao et al., 2011; Zou et al., 2013; Zhang et al., 2017; Assi and Bearman, 2018). More generally span-wise variations of geometry or flow characteristics are at the first order equivalent to diameter variations.

Simulation of VIV can be done by using reduced order models such as wake oscillator models (Païdoussis et al., 2010). In this approach, the wake dynamics is presented by a single variable that satisfies a van de Pol equation. This is coupled to the dynamics of the cylinder see for instance Facchinetti et al. (2004a) where it has been shown that the acceleration coupling is the most appropriate forcing of the bluff body. By using this nonlinear coupled system the main features of VIV phenomenology can be reproduced. This model has been applied to a large variety of cases with non-uniform flows with rigid cylinder and flexible tensioned cable (Mathelin and De Langre, 2005; Srinil et al., 2009; Violette et al., 2007; Xu et al., 2008). The first use of a wake oscillator model to study VIV of tapered cylinders was done by Balasubramanian and Skop (1996), but the drop in amplitude for high tapering was not recovered. The wake oscillator model has also been used to study the response of a tensioned cable subjected to flow with different velocity profiles and different boundary conditions. The results showed that the simple wake oscillator model can model the important features of dynamics of long cylinders such as waves generated in cables. De Langre

* Corresponding author. LadHyX, Ecole polytechnique, Institut polytechnique de Paris, CNRS, Palaiseau, France.
E-mail address: bahramiasl@ladhyx.polytechnique.fr (S. Bahramiasl).

https://doi.org/10.1016/j.oceaneng.2020.108446
Received 28 June 2020; Received in revised form 24 November 2020; Accepted 29 November 2020

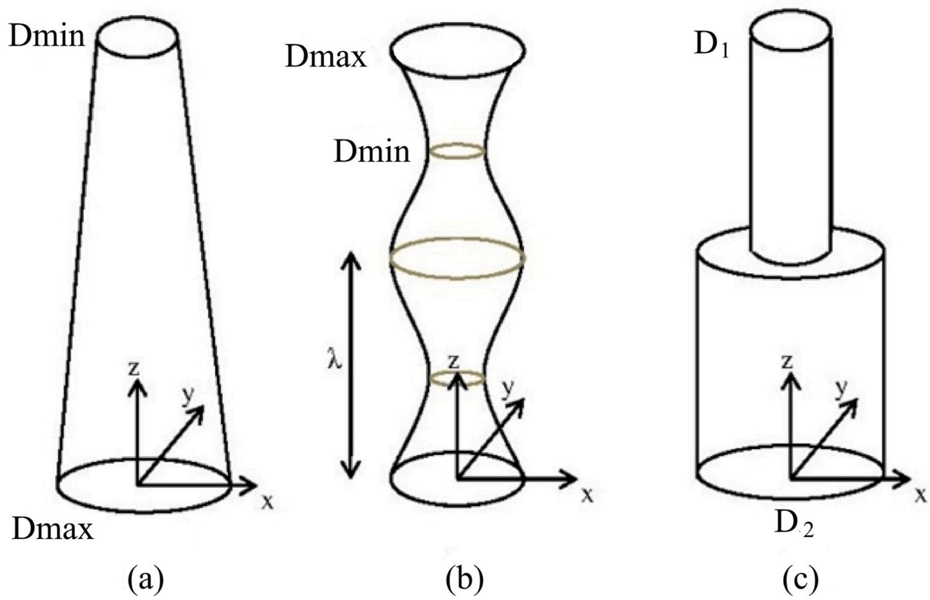

Fig. 1. Cylinders with span-wise variations of cylinders considered in this paper: (a) tapered circular (b) wavy (c)2-section cylinder.

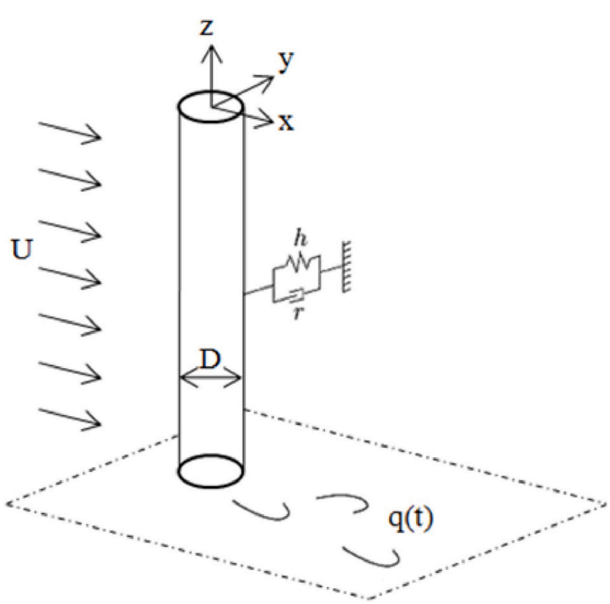

Fig. 2. Elastically supported cylinder subjected to uniform cross flow.

(2006) used a linear stability analysis to analyze the lock-in mechanism VIV. The linear stability analyses of the coupled equations have also been applied to waves generated in the cable. The cable under non-uniform flow and the competition of unstable wave systems have been discussed as well (De Langre, 2006; Gao et al., 2018, 2019; Violette et al., 2007, 2010). Xu et al. (2008) considered the applicability of the nonlinear wake oscillator to high aspect ratio risers and performed experiment to validate their numerical results.

In the present paper we analyze the response of cylinders with different cross sections in three steps. First, we apply the wake oscillator approach of Facchinetti et al. (2004a) to the case of tapered cylinders and wavy cylinders, in the scope of predicting the reduction of amplitude of VIV that occurs, for strong variation of diameters, as a kind of loss of lock-in. A simpler case of a two-section cylinder is then analyzed. In a second approach, based on De Langre (2006), we perform a linear stability analysis of the coupled wake-structure system. This allows finding approximations of the range of flow velocity where lock-in occurs. Finally, in a third approach, as an extension of the linear stability approach, a simple criteria for loss of lock-in is proposed. Section 2 presents the wake oscillator approach, Section 3 the application for different cylinders shown in Fig. 1 Section 4 describes the linear stability analysis and the simple criteria.

2. Wake oscillator model

In this section we recall the main features of the wake oscillator model in Facchinetti et al. (2004a) and we extend it to the case of varying cross section. The van der Pol wake oscillator model has been used for describing the dynamics of the wake behind the cylinder as

$$\frac{\partial^2 q}{\partial t^2}+\varepsilon\left(q^2-1\right)\frac{\partial q}{\partial t}+q=f. \tag{1}$$

Here $q(t)$ is the dimensionless wake variable which is associated to the transverse unsteady lift force, $q=2C_L/C_{L0}$ where C_L is the lift coefficient, and C_{L0} is the reference lift coefficient in a fixed structure subjected to the vortex shedding. In Eq. (1) f is the effect of the motion of the cylinder on the fluid wake oscillator. This can be written as $A\partial^2 Y/\partial t^2$. Here A and ε are parameters that have been determined from experiments for circular cylinders (Facchinetti et al., 2004a). In Fig. 2, an elastically supported rigid cylinder is shown, with diameter D and mass m subjected to a steady uniform flow of velocity U. This body is restricted to have only movement in the cross-flow direction y. The movement of the cylinder can be described by a linear oscillator

$$m\frac{\partial^2 Y}{\partial T^2}+r\frac{\partial Y}{\partial T}+hY=S, \tag{2}$$

where Y is the displacement of the cylinder, m is the total mass of the system which includes the mass of structure and the fluid added mass. Here h is the stiffness of system, r is the total damping modeling both the viscous dissipation $r_s=2m\zeta\Omega_s$ and the added damping $r_f=\gamma/\mu m\Omega_f$ see (Facchinetti et al., 2004a). We define the parameters ζ as the structure reduced damping, $\Omega_s=\sqrt{h/m}$ the natural frequency of the structure, $\gamma=C_D/4\pi St$ as the stall parameter related to the drag coefficient (C_D), Ω_f the frequency of vortex shedding, $\mu=m/\rho D^2$ the mass ratio, $M=C_{L0}/16\pi^2 St^2\mu$ the mass number, St the Strouhal number and finally S the exerted force from vortex to cylinder. In dimensionless form the coupled

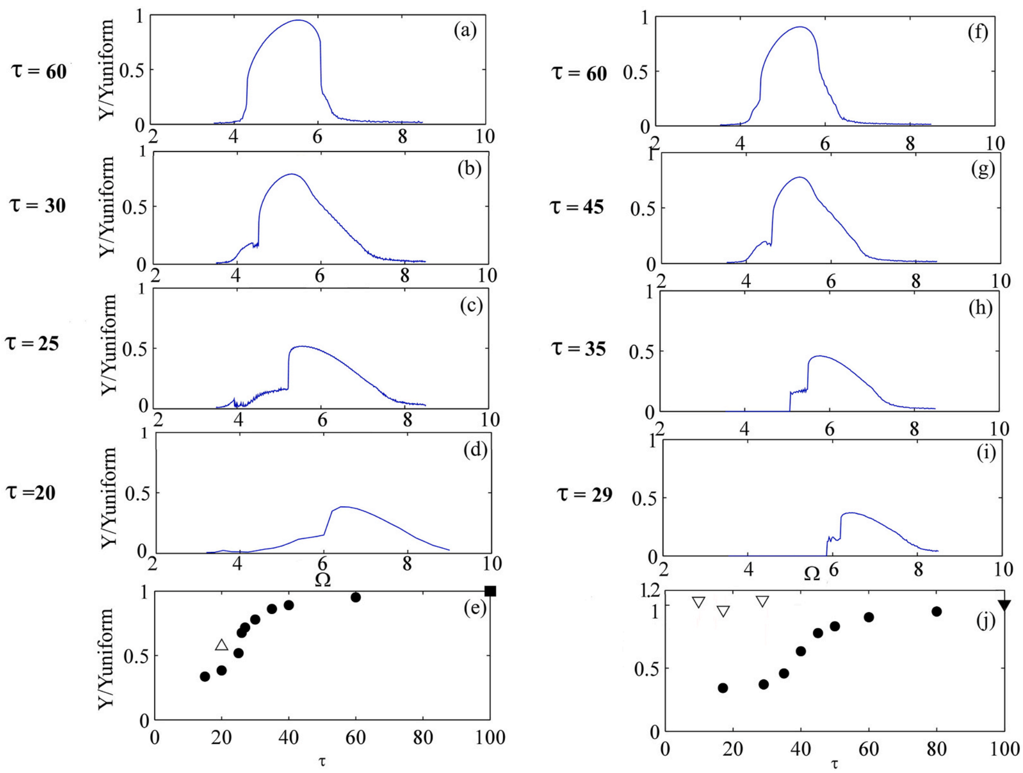

Fig. 3. Effect of tapering ratio τ on the amplitude of VIV of a tapered cylinder. Normalized amplitude of cylinder motion showing a decrease of amplitude when the tapering ratio is reduced (Left; parameters from (Zeinoddini et al., 2013), right; parameters from (Seyed-Aghazadeh et al., 2015)). Last row: maximum amplitude as a function of the tapering ratio τ. The experimental data of Zeinoddini et al. (2013) for uniform and tapered are also shown as ■ and Δ respectively and the experimental data of Seyed-Aghazadeh et al. (2015) for uniform and tapered are shown as ▼ and ▽ respectively.

equations for a uniform cylinder are (Facchinetti et al., 2004a)

$$\begin{cases} \dfrac{\partial^2 y}{\partial t^2} + \left(2\zeta + \dfrac{\gamma}{\mu}\Omega\right)\dfrac{\partial y}{\partial t} + y = M\Omega^2 q \\ \dfrac{\partial^2 q}{\partial t^2} + \varepsilon\Omega\left(q^2 - 1\right)\dfrac{\partial q}{\partial t} + \Omega^2 q = A\ddot{y}. \end{cases} \tag{3}$$

We can extent this formulation to a spanwise varying diameter $D(z)$ as

$$\begin{cases} \dfrac{\partial^2 y}{\partial t^2} + 2\zeta\dfrac{\partial y}{\partial t} + y = \displaystyle\int_{z=0}^{\lambda}\left[M\Omega^2 d(z) q - \dfrac{\gamma}{\mu}\Omega\dfrac{\partial y}{\partial t}\right]dz \\ \dfrac{\partial^2 q}{\partial t^2} + \varepsilon\dfrac{\Omega}{d(z)}\left(q^2 - 1\right)\dfrac{\partial q}{\partial t} + \left(\dfrac{\Omega}{d(z)}\right)^2 q = A\ddot{y} \end{cases} \tag{4}$$

Here $d(z) = D(z)/D_0$, $y = Y/D_0$ is the dimensionless amplitude, D_0 is the mean diameter of the cylinder, $t = T\Omega_s$ is the dimensionless time, $\lambda = L/D_0$ is the dimensionless length and $\Omega = \Omega_f/\Omega_s = (USt/D_0)/\Omega_s = StU_r$ is the reduced angular frequency. Here $q(z,t)$ and $d(z)$ depend on the spanwise coordinate z. Eq. (4) can be solved numerically in time as in the research of Facchinetti et al. (2004a), but with a series of wake oscillator in the spanwize direction see (Facchinetti et al., 2002). The limit cycle in terms of its amplitude that is reached after a transient from a non-zero initial condition, is then analyzed as a function of the parameters, $\Omega = StU_r$ the shedding frequency, and $\tau = L/(D_{max} - D_{min})$ (Mathelin and De Langre, 2005) the tapering ratio for the tapered cylinder and for the wavy cylinder, the ratio (D_{max}/D_{min}) and the wavelength.

It was shown that taking into account the diffusion of the wake dynamics in the spanwise direction did not affect significantly the results (Facchinetti et al., 2002; Mathelin and De Langre, 2005).

The validation of the van der Pol wake oscillator model has been the topic of many papers. Balasubramanian et al. (1996) used nonlinear diffusively coupled wake oscillators to study uniform cylinders and cones under different flow conditions and validated their results against experimental results. In Facchinetti et al. (2002) the wake oscillator approach was used to model the time evolution of vortex shedding over a wavy cylinder in relation to the work of Balasubramanian and Skop (1996) and Bearman and OWen (1998). Facchinetti et al. (2004a) studied the coupling of the wake oscillator with a single structural oscillator and compared the results with experiments and other models. Cables with different conditions have also been studied and the results validated against experiments (Facchinetti et al., 2004b; Violette et al., 2007, 2010). More recently, cables and risers have been modeled using wake oscillators and the results compared with experiments and DNS (Gao et al., 2018, 2019; Lin et al., 2009; Xu et al., 2008). All the comparisons with experiments or CFD have shown that the wake oscillator can represent qualitatively most of the features of VIV, and qualitatively some aspects. Considering its simplicity it is now used in many applications as well as in the analysis of the dynamics of these systems.

3. Loss of lock-in

3.1. Tapered cylinder

We first apply Eq. (4) to the tapered cylinder case corresponding to the experiments of Zeinoddini et al. (2013) ($\mu = 6.1; \lambda = 14.28$). Fig. 3 (a)–(d) shows the normalized amplitude of VIV as a function of $\Omega = StU_r$ for four different levels of tapering. In those figures, the amplitude of vibration of cylinders have been normalized with the amplitude of uniform cylinder with the same characteristics and have been indicated by $Y/Yuniform$. At $\tau = 60$ and $\tau = 30$ the lock-in is similar to that of a uniform cylinder. In those cases ($\tau = 60$ and $\tau = 30$), most of the cylinder is near the diameter at which lock-in occurs. For $\tau = 25$ and $\tau = 20$ the amplitude is much smaller because only a part of the cylinder has a diameter corresponding to the lock-in condition. By systematically exploring the values of τ the evolution of the maximum of the response curve can be plotted, Fig. 3(e). A sharp change at $\tau \simeq 27$ is observed, corresponding to unlock-in. We can define a critical value of the tapering ratio were unlock-in occurs by the center of the S-shaped curve, or the point of maximum slope, here at $\tau = 27$. The experimental data by Zeinoddini et al. (2013) for uniform and tapered at $\tau = 20$ are also shown in Fig. 3(e) as ■ and Δ respectively. The same analysis can be

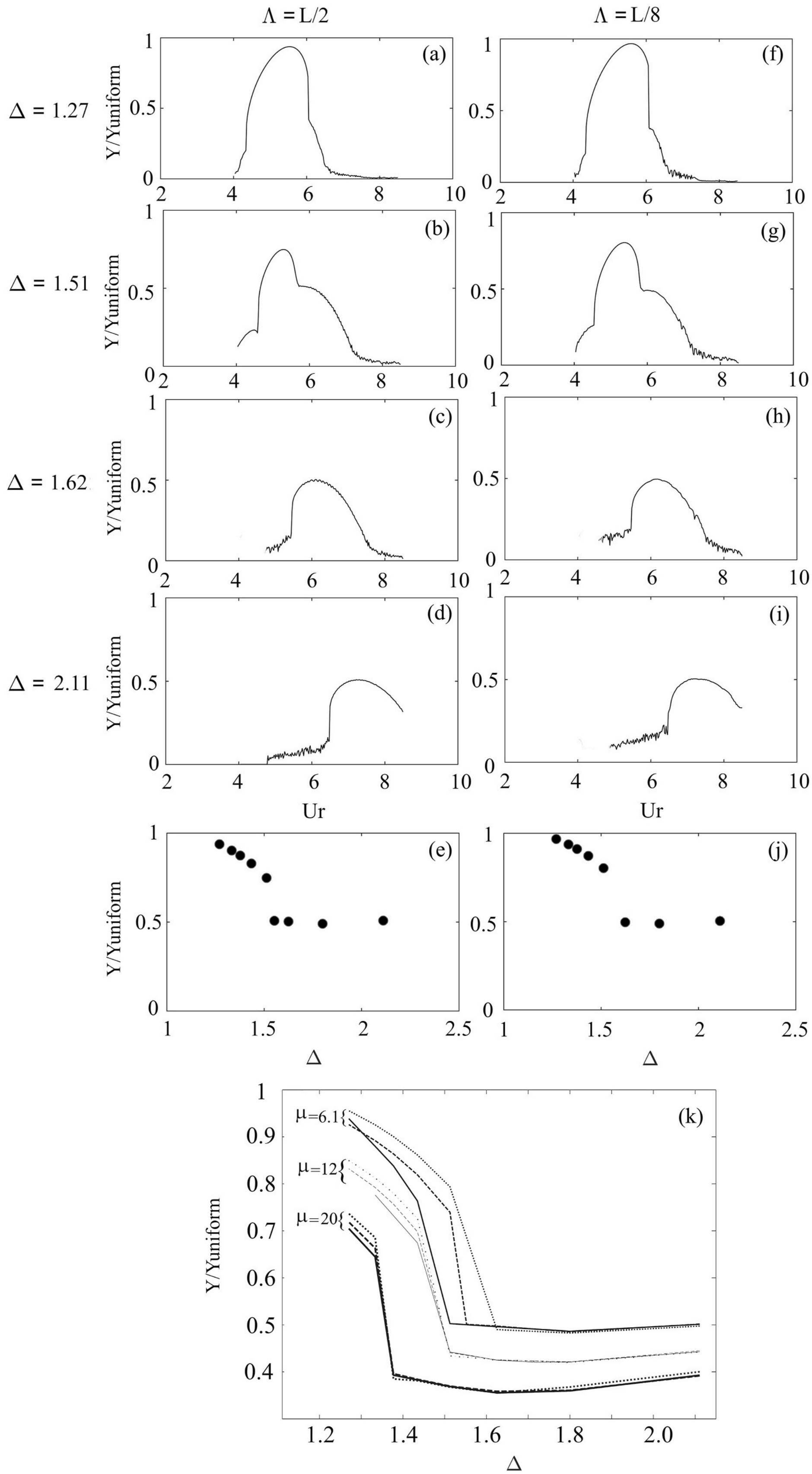

Fig. 4. Effect of diameter ratio Δ on the amplitude of VIV of a wavy cylinder. Normalized amplitude of cylinder motion showing a drop in amplitude as the diameter ratio is increased ((a)–(d): $\Lambda = L/2$; (f)–(i): $\Lambda = L/8$); (e),(j): amplitude as a function of the diameter ratio Δ; (k): effect of wavelength on the response of cylinders with different mass ratio. For each case three wave length are considered, $\Lambda = L/2, L/4, L/8$.

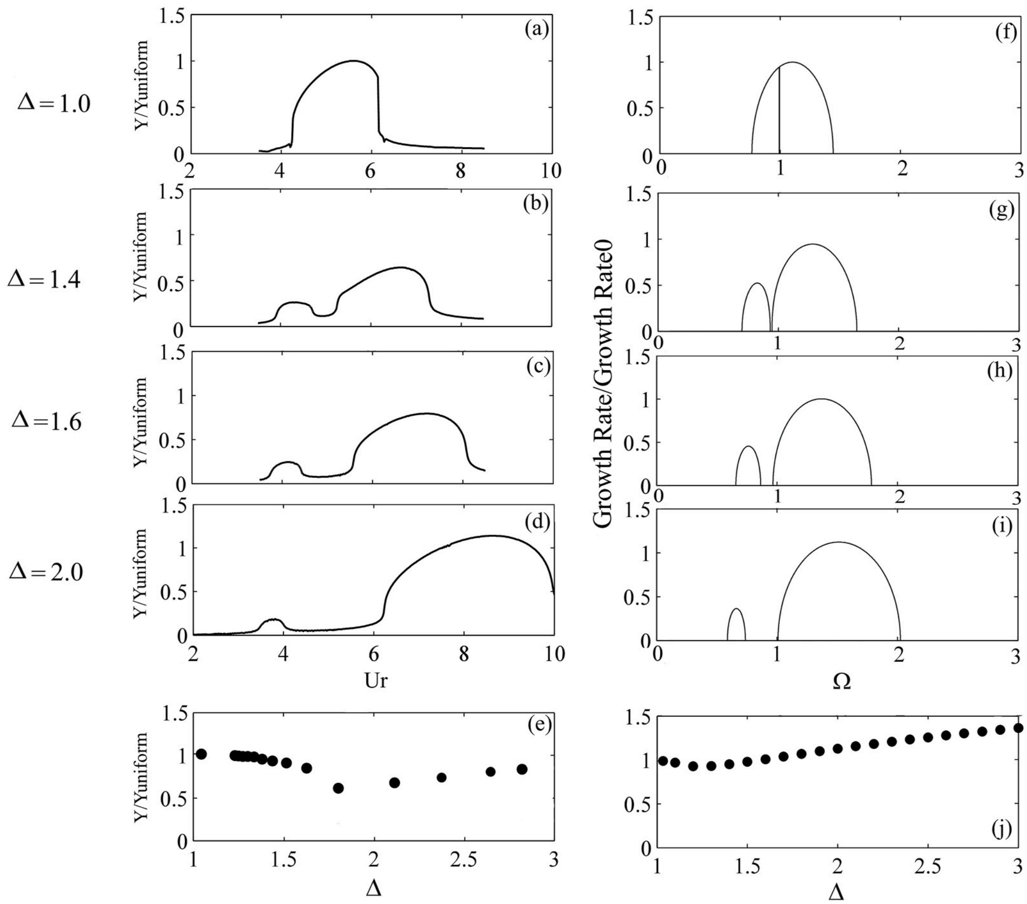

Fig. 5. Left: Effect of diameter ratio Δ on the amplitude of VIV of a two-section cylinder. Normalized amplitude of cylinder motion showing a drop in amplitude as the diameter ratio is increased (left: using nonlinear wake oscillator model; right: using linear stability method); Last row: amplitude as a function of the diameter ratio Δ.

done for the case studied in (Seyed-Aghazadeh et al., 2015) ($\mu = 7.6$; $\lambda = 19.61$). A similar unlock-in is observed at about $\tau = 40$, Fig. 3 right. The change in these two cases show that the strong decrease of VIV amplitude occurs when the tapering is strong enough (low tapering ratio). The critical tapering ratio where the shift occurs seems to depend on mass ratio, which differs between the two cases. The experimental data of Seyed-Aghazadeh et al. (2015) is also shown in Fig. 3(j) as ▽ and ▼ for tapered and uniform cylinders respectively, but do not show any apparent loss of lock-in.

3.2. Wavy cylinder

For wavy cylinders, Fig. 1(b)., another parameter is used to describe the spanwise variation of the diameter, the diameter ratio $\Delta = D_{max}/D_{min}$. The mass ratio and the length to mean diameter ratio are set to 6.1 and 14.28 respectively, as in the first case of tapered cylinder above. The wavelength of the sinusoidal variation of the diameter is set to $L/2$ or $L/8$. Fig. 4 shows the evolution of the amplitude of motion with the diameter ratio Δ. By increasing the variation of diameter the maximum amplitude of oscillation decreases and shifts to higher reduced velocity as in the tapered cases. In both wavy cylinders a drop of amplitude is found, near $\Delta = 1.5$. Note that this drop of amplitude depends on the mass ratio, but weakly on the wavelength of diameter variation except for low mass ratio, as is illustrated Fig. 4(k).

3.3. Two-section cylinder

To gain a better understanding of the drop in VIV amplitude found for the two systems above, we consider the simpler, more generic case, of a two-section cylinder, see Fig. 1(c). Now the diameter ratio Δ is simply the ratio of the two diameters. For that case, the wake variable $q(z,t)$ reduces to two variables $q_1(t)$ and $q_2(t)$, so that Eq. (4) become

$$\begin{cases} \dfrac{\partial^2 y}{\partial t^2} + \left(2\zeta + \dfrac{\gamma}{\mu}\Omega\right)\dfrac{\partial y}{\partial t} + y = M\Omega^2\left(\dfrac{q_1 d_1 + q_2 d_2}{2}\right) \\[2ex] \dfrac{\partial^2 q_1}{\partial t^2} + \varepsilon\dfrac{\Omega}{d_1}(q_1^2 - 1)\dfrac{\partial q_1}{\partial t} + \left(\dfrac{\Omega}{d_1}\right)^2 q_1 = A\dfrac{\partial^2 y}{\partial t^2} \\[2ex] \dfrac{\partial^2 q_2}{\partial t^2} + \varepsilon\dfrac{\Omega}{d_2}(q_2^2 - 1)\dfrac{\partial q_2}{\partial t} + \left(\dfrac{\Omega}{d_2}\right)^2 q_2 = A\dfrac{\partial^2 y}{\partial t^2} \end{cases} \quad (5)$$

where d_1 and d_2 are the upper and lower diameter ratios respectively. The aforementioned equations are solved for this case and the results are represented in Fig. 5.

Fig. 5(a)–(d) show the evolution of the VIV response when the diameter ratio is increased. The classical lock-in response curve, Fig. 5 (a), shifts to a double lock-in curve, Fig. 5(d) for higher diameter ratios. In-between, the amplitude is reduced as no common frequency of lock-in can be found. Fig. 5(e) represents the amplitudes of motion as a function of the diameter ratio. Clearly, the splitting of the lock-in response in two separated lock-in responses results in a drop of the amplitude of response, here near $\Delta = 1.75$. This is similar to the cases of a tapered or wavy cylinder shown before: as the ratio between diameters along the cylinder becomes larger, no common lock-in is found for the coupled dynamical system, and this results in a drop of amplitude. There is a similarity in the shifting to the double lock-in situation for the two-

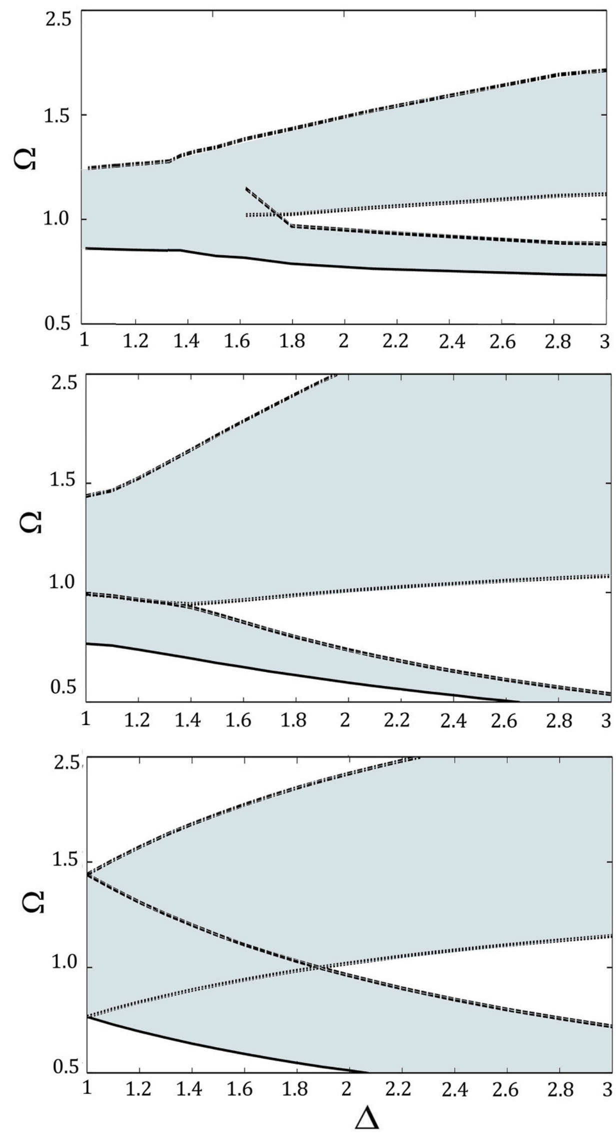

Fig. 6. Effect of the diameter ratio on the range of lock-in in VIV of a two-section cylinder. The range of reduced frequency Ω where lock-in occurs is shaded in grey. (a) full non-linear model, Eq. (5), (b) linear stability analysis of the same system, (c) envelopes of lock-in defined by the simple criteria of Eq. (8).

section and the wavy cylinders. When considering the distribution of diameters, a large part of the wavy and two-section cylinders have a diameter close to the extreme values. Conversely, the tapered cylinder has a uniform distribution of diameters. So, the wavy cylinders and the two-section cylinder have similar behaviors as we can observe in the second row of Fig. 4.

4. A simple criteria for loss of lock-in

In the results of the cases computed above it appears that the amplitude of VIV drops when the ratio between diameters along the cylinder becomes too large. In the tapered cylinder and the wavy cylinder a strong diameter ratio results in a very strong drop of amplitude. For the two-section cylinder, the amplitude of motion is not so strongly reduced, as new lock-in ranges reappear for high diameter ratios.

It seems that the mechanism at the origin of amplitude decrease with non-uniform diameters is related to the inability of the dynamical system to accommodate with wakes of too different natural frequencies. This can be analyzed on the simpler system of the two-section cylinder. In that case, two wake variables coexist, that are governed by wake oscillator equations with two distinct frequencies, see Eq. (5).

We now use the approach of a linear stability analysis of the set of coupled equations, following the work of De Langre (2006). In that approach, the modes of the coupled system, made linear, are computed, and it has been shown that lock-in of the full non-linear system corresponds to the existence of an unstable mode in the linear stability analysis. In the simple case of uniform flow, the range of lock-in can be easily computed (see in Appendix) and reads

$$\frac{1}{1+\sqrt{AM}} < \Omega < \frac{1}{1-\sqrt{AM}}. \tag{6}$$

In the more general case of the two-section cylinders, following the research work of De Langre (2006) we remove from Eq. (5) the non-linear terms and the damping terms. They become

$$\begin{cases} \dfrac{\partial^2 y}{\partial t^2} + y = M\Omega^2\left(\dfrac{q_1 d_1 + q_2 d_2}{2}\right) \\ \dfrac{\partial^2 q_1}{\partial t^2} + \left(\dfrac{\Omega}{d_1}\right)^2 q_1 = A\dfrac{\partial^2 y}{\partial t^2} \\ \dfrac{\partial^2 q_2}{\partial t^2} + \left(\dfrac{\Omega}{d_2}\right)^2 q_2 = A\dfrac{\partial^2 y}{\partial t^2} \end{cases} \tag{7}$$

By looking for eigenmodes in the form of $(y, q_1, q_2) = (y^0, q_1^0, q_2^0)e^{iwt}$, the stability of modes can be assessed by looking at the sign of their growth rate, $-Im(\omega))/Real(\omega))$, see Appendix. Fig. 5(f)–(i) shows the evolution of the growth rates with the parameter Ω, for different diameter ratios Δ, using the same mass ratio as in Fig. 5(a)–(e). For small values of the diameter ratio $\Delta < 1.4$ an unstable mode, corresponding to lock-in, exists in a continuous range of Ω. For higher diameter ratio, two distinct ranges of instability are found. A comparison with the dynamics of the non-linear system, Fig. 5(a)–(e) shows that the linear stability captures the separation of one lock-in in two different ones, which was found to be causing a decrease in amplitude.

To further understand this splitting of the two lock-ins, using Eq. (7), the range of instability of each mode can be approximated considering that it is decoupled, in the interaction with the cylinder, of the other mode. They would read respectively

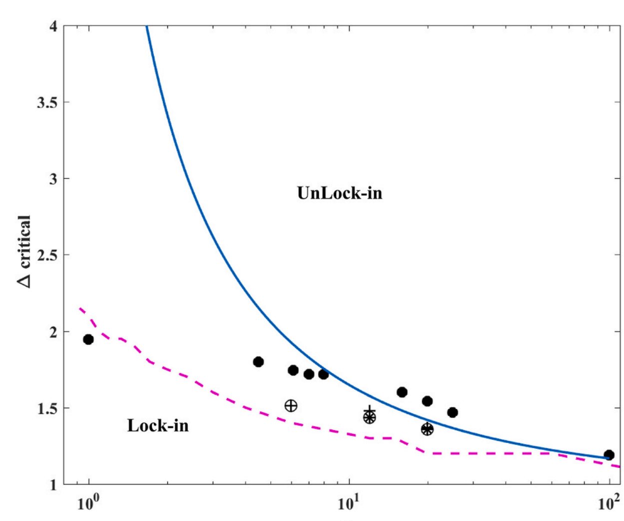

Fig. 7. Critical diameter ratio for loss of lock-in. Non-linear computations, Section 3: • tapered cylinder; *,o,+ wavy cylinder with $\Lambda = L/2, L/4, L/8$ respectively. Linear stability analysis of the two-section cylinder, dashed line. Simplified criteria based on the linear range of lock-in, Eq. (10), continuous line.

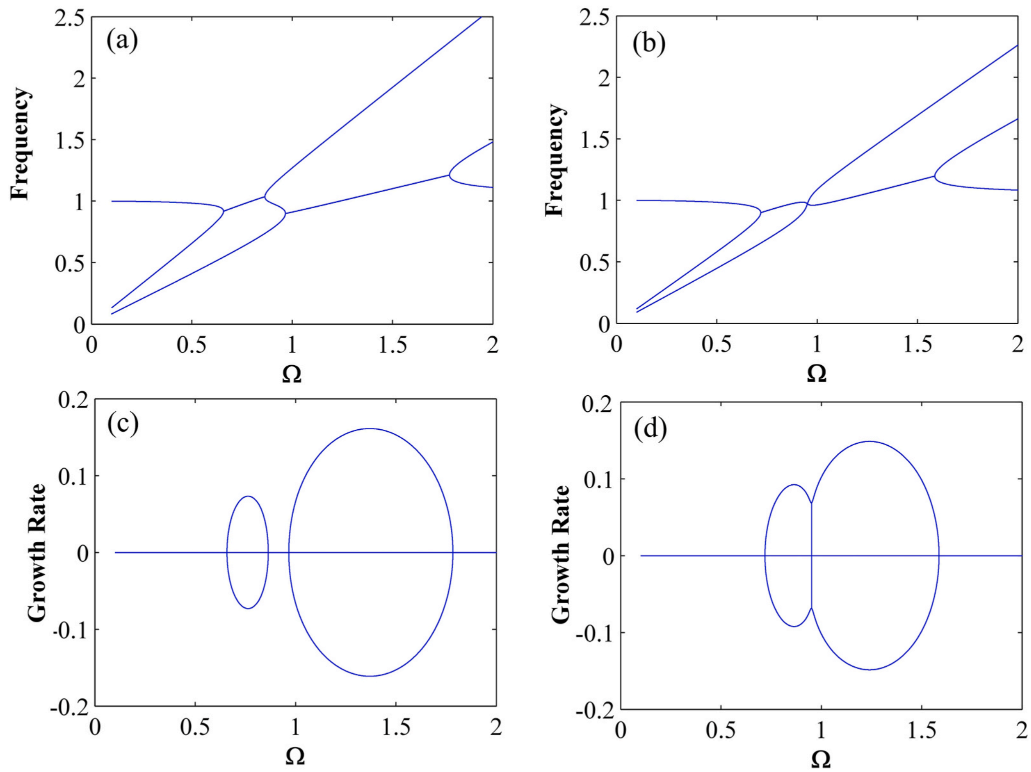

Fig. 8. Results of the linear stability analysis for the two-section cylinder. (a) frequency for $\Delta = 1.6$; (b) frequency for $\Delta = 1.3$; (c) Growth rate for $\Delta = 1.6$; (d) Growth rate for.$\Delta = 1.3$

$$\begin{cases} \dfrac{1}{1+\sqrt{AM}} < \dfrac{\Omega}{d_1} < \dfrac{1}{1-\sqrt{AM}} \\ \dfrac{1}{1+\sqrt{AM}} < \dfrac{\Omega}{d_2} < \dfrac{1}{1-\sqrt{AM}}. \end{cases} \tag{8}$$

Fig. 6 shows the evolution of the lock-in range with Δ, for the same mass ratio $\mu = 6.1$, with the three approaches above: (a) the solution of the full non-linear Eq. 5, (b) the linear stability analysis of Eq. (7) and (c) Eq. (8). It is shown that the linear stability approach, as well as the simple approximation of Eq. (8) capture reasonably well the effect of Δ on lock-in.

Let us now propose a simple criteria for loss of lock-in when diameters vary, based on the results above. These two regions of lock-in defined by Eq. (8) will be separated if the lower bound of the higher domain is larger than the upper bound of the lower domain:

$$\frac{d_1}{1-\sqrt{AM}} < \frac{d_2}{1+\sqrt{AM}} \tag{9}$$

or, equivalently in term of diameter ratio and mass ratio

$$\Delta = \frac{1+\sqrt{\frac{AC}{\mu}}}{1-\sqrt{\frac{AC}{\mu}}}. \tag{10}$$

where $C = C_{L0}/(16\pi^2 St^2)$. In Fig. 7, for all the cases considered in this paper, we can plot the critical diameter ratio that causes a drop in amplitude, as a function of the mass ratio μ. The criterion defined by Eq. (10) gives a good approximation of the critical diameter ratio, except for small mass ratio. Note that the linear stability analysis presented above for the two-section cylinder gives a more conservative prediction.

5. Discussion and conclusion

We have focused here on the particular case of a uniform flow on a cylinder with varying cross-section, and used a simple model of the interaction between the wake and the cylinder to try and derive a first understanding of the role of the parameters.

In all the cases we have studied, where the cylinder was tapered, wavy or with two-section, a common featured was found in the results of the computations of VIV: the amplitude of response decreased when the ratio between the maximum and minimum diameter increased. The full lock-in that occurs when the diameter is uniform enough is lost. By using a simple linear stability analysis, the loss of lock-in can be understood as the inability of the dynamical system to simultaneously accommodate with very different wake oscillators, which are the driving force of VIV. This simple idea can be expressed in a criterion, Eq. (10), which is derived from previous studies on a linear stability approach of VIV. The comparison with the results of all the computed cases show that the main effects are well captured, mainly through the effect of the mass ratio. Eq. (10) is probably applicable to other shapes of cylinders, considering that we have analyzed here different shapes (tapered, two-section and wavy) with a large range of mass ratio. The applicability to the general case of cables with a variable flow profile is under current analysis.

Going back to the more general problem of spanwise variations, it is possible to use the present results to address the issue of variations of flow velocity, or even simultaneous variations of flow velocity and diameter. The more general form of Eq. (10) would read

$$\frac{(d/u)_2}{(d/u)_1} = \frac{1+\sqrt{\frac{AC}{\mu}}}{1-\sqrt{\frac{AC}{\mu}}}. \tag{11}$$

These results would now need to be checked with a much larger set of data, including experiments and full solutions of the fluid dynamics coupled with the cylinder dynamics. Presently, no systematic studies give values of critical diameter ratio although the literature cited in the Introduction shows a decrease in amplitude when the span-wise variations of diameters increase. This is a field of current research.

Declaration of competing interest

The authors declare that they have no known competing financialinterestsor personal relationships that could have appeared to influence the work reported in this paper.

Appendix A

In the linear stability analysis by De Langre (2006) the damping terms in the equations have been neglected and the modes considered as: $(y,q) = (y_0,q_0)e^{i\omega t}$. So Eq. (3) become:

$$\begin{cases} -y_0\omega^2 + y_0 = M\Omega^2 q_0 \\ -q_0\omega^2 + q_0 = -Ay_0\omega^2. \end{cases} \tag{12}$$

Consequently, the frequency equation has been obtained as

$$\omega = \sqrt{\frac{1+(1-AM)\Omega^2 \pm \sqrt{[1+(1-AM)\Omega^2]^2 - 4\Omega^2}}{2}} \tag{13}$$

and solved. It has been found that the range $1/1+\sqrt{AM} < \Omega < 1/1-\sqrt{AM}$ corresponds to the situation when two modes are coincide so the lock-in occurs. This procedure has been done for the case of two-section cylinder and the equation of frequency is obtained by Eq. (7) as below:

$$\omega^6 + \omega^4\left(\Omega^2(AM-S)-1\right) + \omega^2\left(\Omega\left(S+\Omega^2 H - \Omega^2 AMP\right)\right) - \Omega^4 H = 0 \tag{14}$$

where $S = (\Delta^2+1)(\Delta+1)^2/4\Delta^2$, $H = (\Delta+1)^4/16\Delta^2$ and $P = (\Delta+1)^4(2+6((\Delta-1)/(\Delta+1))^2)/16\Delta^2$. The solution of this frequency equation, for a given value of Δ, gives three solutions at a given value of Ω. This is illustrated Fig. 8. The case of high diameter ratio (left) shows twice the simple linear lock-in mechanism described by De Langre (2006) where two (real) frequencies merge into one, with a positive grow rate: this happens in two separate ranges of Ω, corresponding to lock-in between the wakes of each sections with the cylinder mode. Conversely, Fig. 8 right shows a case of low diameter ratio where the lock-in process is continuous between the two ranges of Ω.

References

Assi, G.R., Bearman, P.W., 2018. Vortex-induced vibration of a wavy elliptic cylinder. J. Fluid Struct. 80, 1–21.
Balasubramanian, S., Skop, R., 1996. A nonlinear oscillator model for vortex shedding from cylinders and cones in uniform and shear flows. J. Fluid Struct. 10 (3), 197–214.
Bargi, K., Tamimi, V., Zeinoddini, M., 2015. Viv of tapered cylinders: 3D LES numerical simulation. Int. J. Maritime Technol. 3, 17–31.
Bearman, P.W., OWen, J.C., 1998. Reduction of bluff-body drag and suppression of vortex shedding by the introduction of wavy separation lines. J. Fluid Struct. 12 (1), 123–130.
De Langre, E., 2006. Frequency lock-in is caused by coupled-mode flutter. J. Fluid Struct. 22 (6–7), 783–791.
Facchinetti, M.L., de Langre, E., Biolley, F., 2002. Vortex shedding modeling using diffusive van der pol oscillators. Compt. Rendus Mec. 330 (7), 451–456.
Facchinetti, M.L., De Langre, E., Biolley, F., 2004a. Coupling of structure and wake oscillators in vortex-induced vibrations. J. Fluid Struct. 19 (2), 123–140.
Facchinetti, M.L., de Langre, E., Biolley, F., 2004b. Vortex-induced travelling waves along a cable. Eur. J. Mech. B Fluid 23 (1), 199–208.
Gao, Y., Zong, Z., Zou, L., Takagi, S., 2018. Vortex-induced vibrations and waves of a long circular cylinder predicted using a wake oscillator model. Ocean Eng. 156, 294–305.
Gao, Y., Zou, L., Zong, Z., Takagi, S., Kang, Y., 2019. Numerical prediction of vortex-induced vibrations of a long flexible cylinder in uniform and linear shear flows using a wake oscillator model. Ocean Eng. 171, 157–171.
Grouthier, C., Michelin, S., Bourguet, R., Modarres-Sadeghi, Y., De Langre, E., 2014. On the efficiency of energy harvesting using vortex-induced vibrations of cables. J. Fluid Struct. 49, 427–440.
Hover, F., Techet, A., Triantafyllou, M., 1998. Forces on oscillating uniform and tapered cylinders in cross flow. J. Fluid Mech. 363, 97–114.
Kaja, K., Zhao, M., Xiang, Y., Cheng, L., 2016. Three-dimensional numerical simulations of vortex-induced vibrations of tapered circular cylinders. Appl. Ocean Res. 60, 1–11.
Lam, K., Lin, Y., 2009. Effects of wavelength and amplitude of a wavy cylinder in cross-flow at low Reynolds numbers. J. Fluid Mech. 620, 195–220.
Lam, K., Wang, F., So, R., 2004. Three-dimensional nature of vortices in the near wake of a wavy cylinder. J. Fluid Struct. 19 (6), 815–833.
Lee, S.-J., Nguyen, A.-T., 2007. Experimental investigation on wake behind a wavy cylinder having sinusoidal cross-sectional area variation. Fluid Dynam. Res. 39 (4), 292.
Lin, L.-m., Ling, G.-c., Wu, Y.-x., Zeng, X.-h., 2009. Nonlinear fluid damping in structure-wake oscillators in modeling vortex-induced vibrations. J. Hydrodyn., Ser. B 21 (1), 1–11.
Mathelin, L., De Langre, E., 2005. Vortex-induced vibrations and waves under shear flow with a wake oscillator model. Eur. J. Mech. B Fluid 24 (4), 478–490.
Narasimhamurthy, V.D., Andersson, H.I., Pettersen, B., 2009. Cellular vortex shedding behind a tapered circular cylinder. Phys. Fluids 21 (4), 044106.
Païdoussis, M.P., Price, S.J., De Langre, E., 2010. Fluid-structure Interactions: Cross-Flow-Induced Instabilities. Cambridge University Press.
Parnaudeau, P., Heitz, D., Lamballais, E., Silvestrini, J.-H., 2007. Direct numerical simulations of vortex shedding behind cylinders with spanwise linear nonuniformity. J. Turbul. 8, N13.
Seyed Aghazadeh, B., Carlson, D.W., Modarres Sadeghi, Y., 2015. The influence of taper ratio on vortex-induced vibration of tapered cylinders in the crossflow direction. J. Fluid Struct. 53, 84–95.
Srinil, N., Wiercigroch, M., O'Brien, P., Younger, R., 2009. Vortex-induced vibration of catenary riser: reduced-order modeling and lock-in analysis using wake oscillator. In: ASME 2009 28th International Conference on Ocean, Offshore and Arctic Engineering. American Society of Mechanical Engineers Digital Collection, pp. 311–321.
Techet, A., Hover, F., Triantafyllou, M., 1998. Vortical patterns behind a tapered cylinder oscillating transversely to a uniform flow. J. Fluid Mech. 363, 79–96.
Violette, R., De Langre, E., Szydlowski, J., 2007. Computation of vortex-induced vibrations of long structures using a wake oscillator model: comparison with dns and experiments. Comput. Struct. 85 (11–14), 1134–1141.
Violette, R., de Langre, E., Szydlowski, J., 2010. A linear stability approach to vortex-induced vibrations and waves. J. Fluid Struct. 26 (3), 442–466.
Williamson, C., Govardhan, R., 2004. Vortex-induced vibrations. Annu. Rev. Fluid Mech. 36, 413–455.
Xu, W.-H., Zeng, X.-H., Wu, Y.-X., 2008. High aspect ratio (l/d) riser viv prediction using wake oscillator model. Ocean Eng. 35 (17–18), 1769–1774.

Zeinoddini, M., Tamimi, V., Seif, M.S., 2013. Stream-wise and cross-flow vortex induced vibrations of single tapered circular cylinders: an experimental study. Appl. Ocean Res. 42, 124–135.

Zhang, K., Katsuchi, H., Zhou, D., Yamada, H., Zhang, T., Han, Z., 2017. Numerical simulation of vortex induced vibrations of a flexibly mounted wavy cylinder at subcritical Reynolds number. Ocean Eng. 133, 170–181.

Zhao, R., Xu, J.-L., Yan, C., Yu, J., 2011. Scale-adaptive simulation of flow past wavy cylinders at a subcritical Reynolds number. Acta Mech. Sin. 27 (5), 660.

Zou, L., Guo, C., Xiong, C., 2013. Flow characteristics of the two tandem wavy cylinders and drag reduction phenomenon. J. Hydrodyn. 25 (5), 737–746.